

1 Structural Characterization of a Gold/Serum Albumin Complex

2 Alessandro Pratesi,[†] Damiano Cirri,[†] Dolores Fregona,[‡] Giarita Ferraro,[§] Anna Giorgio,[§]3 Antonello Merlino,^{*,§} and Luigi Messori^{*,†}4 [†]Laboratory of Metals in Medicine (MetMed), Department of Chemistry "U. Schiff", University of Florence, via della Lastruccia 3,
5 50019 Sesto Fiorentino, Italy6 [‡]Department of Chemical Sciences, University of Padova, via Marzolo 1, 35131 Padova, Italy7 [§]Department of Chemical Sciences, University of Naples Federico II, via Cinthia, 80126 Napoli, Italy8 **S** Supporting Information

ABSTRACT: The medicinal gold(III) dithiocarbamate complex AuL₁₂ forms a stable adduct with bovine serum albumin. The crystal structure reveals that a single gold(I) center is bound to Cys34, with the dithiocarbamate ligand being released. To the best of our knowledge, this is the first structure for a gold adduct of serum albumin.

Serum albumin (SA) is the most abundant serum protein performing crucial roles in the binding and blood transport of a variety of exogenous substances and drugs.^{1,2} Notably, SA has been reported to be the carrier of several metal ions and metal-containing species in the bloodstream.^{3,4} Although extensive studies have been carried out to characterize the interactions of SA with several metal-based drugs, until now very few structures have been reported for SA/metal drug adducts.^{5,6} In particular, no structure has ever been reported for SA adducts with gold compounds.

AuL₁₂ (Figure 1) is a mononuclear gold(III) complex developed in the group of Dolores Fregona in Padua that has

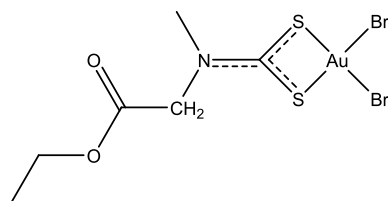


Figure 1. AuL₁₂ structure.

revealed very encouraging cytotoxic and anticancer properties both in vitro and in vivo.^{7,8}

This compound consists of a square-planar gold(III) center with a bidentate dithiocarbamate ligand and two bromide ligands.⁹ Notably, AuL₁₂ has been shown to behave as a prodrug by releasing its bromide ligands. Significant oxidizing properties of the compound were also documented.^{7,8} Previous studies analyzed the interactions of AuL₁₂ with proteins, and also with SA, and offered a general description of the binding process that relies on a redox event.⁸ Here we have explored in more detail the reaction of AuL₁₂ with bovine serum albumin (BSA) and attempted to characterize the products of this reaction at the molecular level. To this end, we have taken advantage of the combined X-ray diffraction (XRD)/electro-

spray ionization mass spectrometry (ESI-MS) protocol recently developed in our laboratories to elucidate protein metalation processes.^{5,10,11}

First, the reaction of AuL₁₂ with BSA was analyzed spectroscopically according to classical methods, and clear evidence was gained for the occurrence of a redox process whereby the gold(III) center undergoes a reduction to gold(I) and the resulting gold(I) ion tightly binds the protein (Figure S1).⁸ Accordingly, the band at 320 nm characteristic of the gold(III) center in AuL₁₂ progressively disappears, and a new band builds up at 380 nm. Further independent evidence for the occurrence of an interaction between AuL₁₂ and BSA has been obtained through other biophysical methods such as circular dichroism (CD; see the Supporting Information, SI).

Afterward, the interaction of AuL₁₂ with BSA was investigated by X-ray crystallography. Good-quality crystals of BSA are difficult to obtain,¹² and the first structure of the protein was solved only in 2012.¹³ At the moment, in the Protein Data Bank, there are only two structures of BSA complexes, one with naproxen¹⁴ and the other with 3,5-diiodosalicylic acid,¹⁵ and there are no structures of adducts with metallodrugs. The crystals of AuL₁₂/BSA diffract X-rays to 3.2 Å resolution using a synchrotron radiation source. Two molecules of BSA are present in the asymmetric unit (a.u.) in this crystal (Figure 2A).¹² The overall structure of the protein is not affected by the reaction with AuL₁₂. Root-mean-square deviations between α -carbon atoms of the adduct and native protein are within the range 0.38–0.45 Å.

Inspection of the electron density in the $F_{\text{obs}} - F_{\text{calc}}$ map allows one to easily identify the presence of a gold atom close to the side chain of Cys34 in both BSA molecules present in the a.u. The presence of the gold center was unambiguously supported by a strong peak in the anomalous difference electron density map (Figure 2B). As a negative control to confirm the binding of gold to Cys34, we compared the electron density of Cys34 in the AuL₁₂/BSA adduct with that of BSA in the absence of any ligands. As supposed, no electron density was observed around the side chain of Cys34 in the structure of BSA, further confirming our assignment.

Close to the gold center, there is no electron density corresponding to the dithiocarbamate ligand; however, because of the low resolution of the structure of the adduct, 82

Received: June 26, 2019

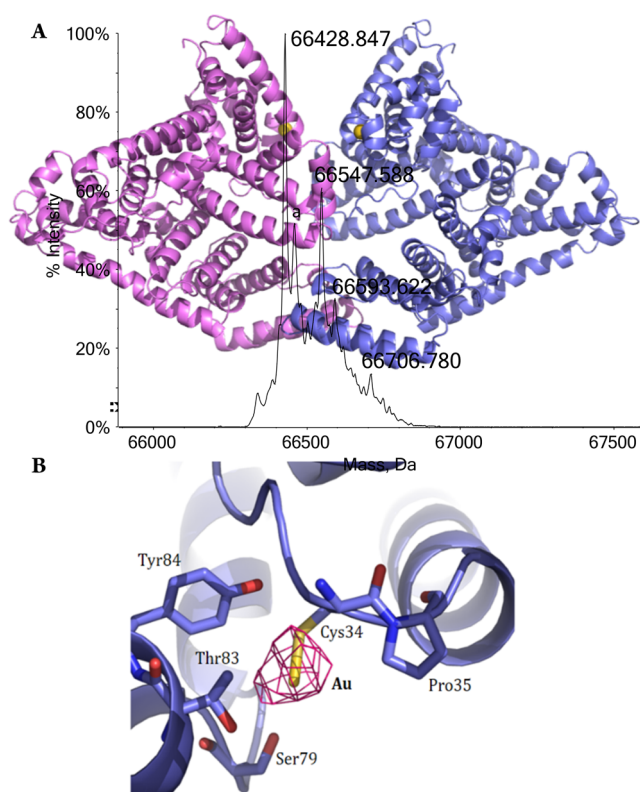


Figure 2. (A) a.u. content of crystals of the AuL₁₂/BSA adduct. The gold atom is indicated as a yellow sphere. (B) Detail of the gold binding site in one of the molecules of the adduct in the a.u. An anomalous difference electron density map corresponding to the gold center is reported at a 3.5 σ value (see also Figure S2).

83 we cannot dismiss that this absence could be due to
84 conformational disorder.

85 Thus, to gain additional and independent data on this
86 system, high-resolution ESI-MS spectra on the AuL₁₂/BSA
87 adduct were collected. We have recently set the best conditions
88 to analyze the intact protein and its interactions with ligands
89 and metallo drugs.^{16–19} Accordingly, the ESI-MS spectrum of
90 BSA in a 20 mM ammonium acetate buffer (pH 6.8) was
91 recorded (Figure 3A).

92 The spectrum exhibits four main peaks that are assigned to
93 native BSA (66428.847 Da) and to its principal physiological
94 post-translational modifications (PTMs), namely, the cystei-
95 nylation of Cys34 (66547.558 Da), an oxidized form of the
96 same residue at 66461.80 Da (Cys-SO₂H), and a signal at
97 66593.622 Da, belonging to a glycosylated form of SA.^{16,20}

98 Subsequently, an aliquot of a AuL₁₂ stock solution in
99 dimethyl sulfoxide (DMSO; maximum DMSO final concen-
100 tration of 5% v/v) was added in a 1:1 protein-to-metal molar
101 ratio to a solution of BSA dissolved in a 20 mM ammonium
102 acetate buffer (pH 6.8). The obtained sample was incubated at
103 37 °C, and the ESI-MS spectrum was recorded after 3 h
104 (Figure 3B). Notably, some new signals appear at higher MWs,
105 marked with blue triangles. In particular, the peaks with
106 molecular masses of 66623.505 and 66818.804 Da nicely
107 correspond to BSA adducts containing 1 or 2 nude gold ions;
108 the peaks of smaller intensity, at 67016.985 and 67210.592 Da,
109 belong to protein adducts containing three and four gold ions,
110 respectively. Moreover, the spectrum also shows a signal at
111 66428.847 Da, corresponding to a small residual amount of
112 unreacted BSA, and two other peaks, corresponding to the

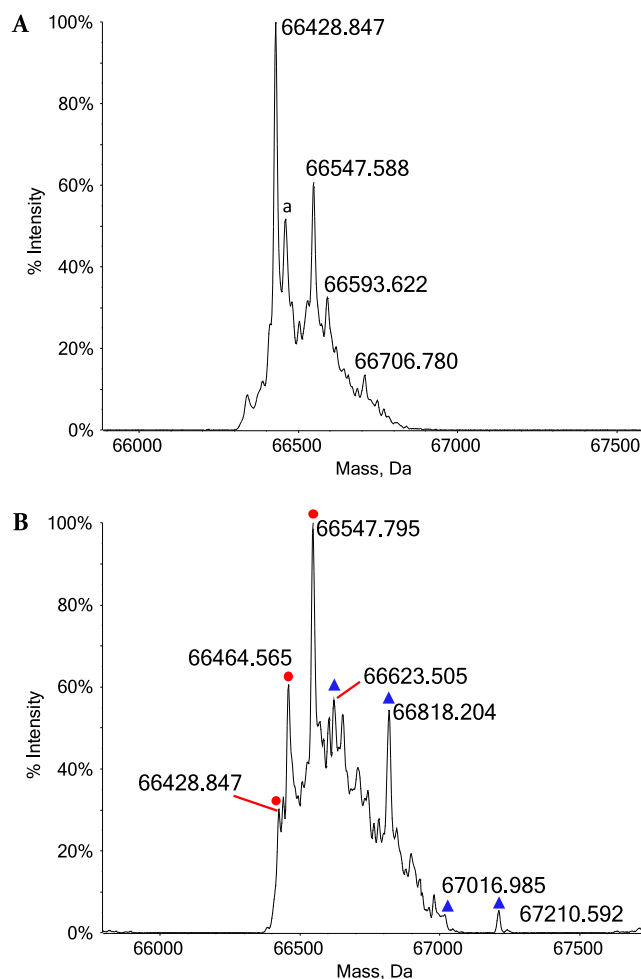


Figure 3. (A) Deconvoluted ESI-MS spectrum of BSA (10^{-5} M) in a 20 mM ammonium acetate buffer (pH 6.8; $a = 66461.80$ Da). (B) Deconvoluted ESI-MS spectrum of the AuL₁₂/BSA mixture. AuL₁₂ was incubated for 3 h with BSA (10^{-4} M) in a 1:1 metal-to-protein molar ratio at 37 °C in a 20 mM ammonium acetate buffer (pH 6.8).

principal PTMs (e.g., sulfenylation and cysteinylolation of
Cys34) of BSA that remain unaltered (signals marked with
red circles). This observation implies that BSA can bind an
increasing amount of AuL₁₂; however, upon protein binding,
AuL₁₂ undergoes an invariant reduction to gold(I) and loses all
its ligands so that only naked gold(I) ions are associated with
the protein. This behavior toward serum proteins under
physiological-like conditions is common for gold(III) com-
plexes and is well documented (i.e., activation by reduc-
tion).^{21–23} As reported in a recent paper, the free thiol group
of Cys34 is the preferential binding site for gold(I) compounds
in BSA.¹⁶ The reaction of gold compounds with BSA gives rise
to mono- or digold adducts on this residue, without any
evidence for the involvement of further binding sites (i.e.,
histidine side chains).¹⁶ Surprisingly, in the case of AuL₁₂, it
is evident that BSA can bind up to four gold atoms. To explain
this behavior, we have hypothesized that AuL₁₂ undergoes
reduction in aqueous solution, leading to the formation of
reactive gold(I) species and to release of the dithiocarbamate
ligand.^{22,23} The presence in an aqueous solution of the
gold(III) complex can cause the oxidative opening of some
disulfide bonds in BSA,²⁴ with subsequent ligation of the
reduced gold(I) species.²⁵ To verify this hypothesis, AuL₁₂ was

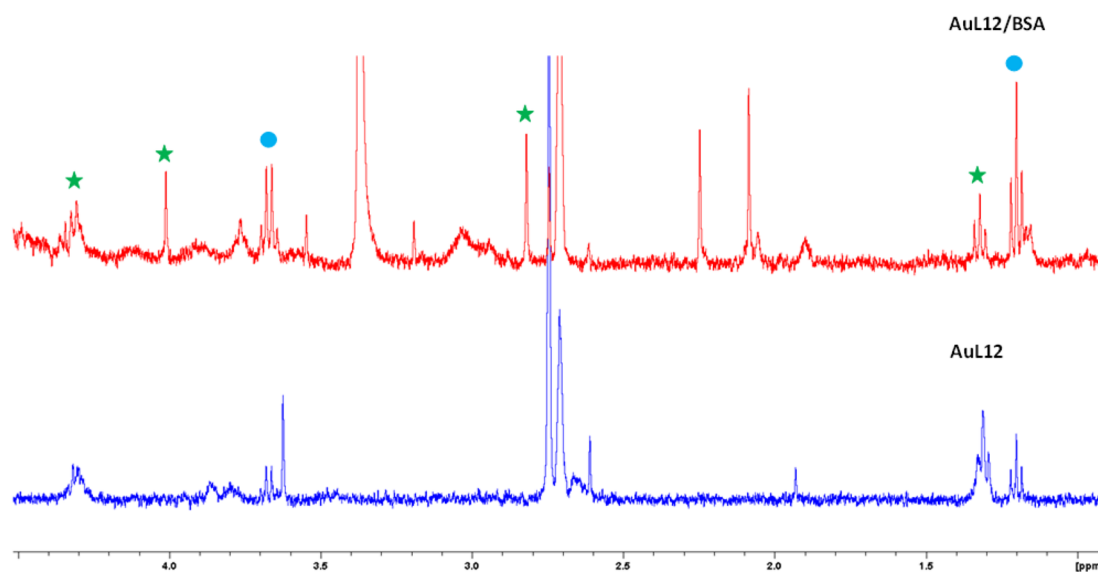


Figure 4. ^1H NMR spectrum of 0.45 mM AuL_{12} in D_2O with 3% $\text{DMSO}-d_6$ (blue). ^1H NMR spectrum of 0.45 mM AuL_{12} incubated with 0.45 mM BSA in D_2O with 3% $\text{DMSO}-d_6$ (red). The acquisitions were performed using a `cpmgpr1d` pulse sequence.

136 reacted with an aqueous solution of cystine and an ESI-MS
137 spectrum recorded. The spectrum shows a principal peak at
138 508.9936 Da (Figures S3–S5) that corresponds to a single
139 gold(III) atom coordinated to one dithiocarbamate moiety
140 and one cysteine residue (see the SI for the isotopic pattern).
141 This evidence perfectly fits with our hypothesis; in fact, the
142 residual gold(III) atom maintains one bond with the
143 dithiocarbamate moiety, while coordination is completed
144 with a cysteinato residue deriving from cleavage of the cystine
145 disulfide bond, stabilizing the gold center in the 3+ oxidation
146 state.²⁵

147 Therefore, the ESI-MS and XRD results are broadly
148 consistent and suggest the occurrence of gold binding to the
149 protein upon gold(III)-to-gold(I) reduction with simultaneous
150 release of the dithiocarbamate ligand. Some ^1H NMR measure-
151 ments were also carried out. ^1H NMR spectra were acquired
152 using a monodimensional CPMG pulse sequence with solvent
153 presaturation (`cpmgpr1d`). This experimental procedure
154 permits one to remove from the ^1H NMR spectra all broad
155 signals originating from nuclei with short T_2 , usually those
156 belonging to large macromolecules (i.e., BSA and BSA/ AuL_{12}
157 adduct in our cases); this typically leads to simpler ^1H NMR
158 spectra only showing the signals belonging to small molecules
159 (or their fragments) in solution.²⁶

160 The ^1H NMR spectrum obtained for the 1:1 AuL_{12} /BSA
161 system is shown in Figure 4; the spectrum of AuL_{12} alone
162 recorded under the same conditions is also reported for
163 comparison. The low signal-to-noise ratio of these ^1H NMR
164 spectra is strictly related to the fact that the optimal BSA
165 concentration (hence, also the AuL_{12} concentration) turned
166 out to be 0.45 mM. Indeed, larger BSA concentrations produce
167 a drastic increase in the viscosity accompanied by a relevant
168 broadening of the NMR signals. Notably, the ^1H NMR
169 spectrum of BSA treated with AuL_{12} reveals several well-
170 detectable signals belonging to low-molecular-weight com-
171 pounds (no such signals are observed in the ^1H NMR
172 spectrum of the protein alone; see the SI). In Figure 4,
173 relatively weak peaks are observed for the signals assigned to
174 AuL_{12} ; in contrast, a few more intense signals are observed that
175 could be assigned to ethyl sarcosinate (δ 4.30, 3.99, 2.79, and

1.29; marked with green stars) and ethanol (δ 3.64 and 1.17; 176
177 marked with cyan circles), which originate most likely from
178 decomposition of the dithiocarbamate ligand. Some additional
179 signals refer to DMSO residual peaks (δ 2.74 and 2.71; see the
180 SI), to BSA impurities (δ 3.34; see the SI), or to ^{13}C couplings
181 (satellite signals at δ 3.52 and 3.16). These results support the
182 concept that AuL_{12} breaks down to a large extent upon
183 interaction with BSA and releases its dithiocarbamate moiety;
184 the latter, in turn, may undergo further degradation processes.

185 Coordinates and structure factors have been deposited in the
186 Protein Data Bank under the accession code 6RJV. These data
187 can be obtained free of charge via www.rcsb.org/.

188 In conclusion, we have succeeded in solving the crystal
189 structure of the AuL_{12} /BSA adduct. The structure reveals some
190 important features; a single gold center binds the protein at the
191 level of the side chain of Cys34, while the overall structure of
192 the protein is not affected. Selective modification of Cys34 by
193 gold coordination is unequivocally demonstrated. Remarkably,
194 when bound to the protein, the gold center has lost its original
195 dithiocarbamate ligand. This concept is strongly supported by
196 independent ESI-MS data showing that a number of naked
197 gold(I) centers are bound to the protein. ^1H NMR
198 measurements point out that the signals of AuL_{12} greatly
199 reduce their intensity in the presence of BSA; in addition, the
200 signals of chemical species deriving from degradation of the
201 dithiocarbamate ligand are clearly seen. Thus, X-ray, ESI-MS,
202 and NMR data nicely concur in drawing a consistent
203 description for the AuL_{12} /BSA adduct. It is worth reminding
204 that this is the first crystal structure for a gold/SA adduct. This
205 structure may be of interest and relevance in relation to the
206 processes of gold nanoparticle formation and assembly assisted
207 by SA, which have attracted a lot of attention in recent years.²⁷

■ ASSOCIATED CONTENT

📄 Supporting Information

The Supporting Information is available free of charge on the
ACS Publications website at DOI: 10.1021/acs.inorg-
chem.9b01900.

- 213 Experimental procedures, additional ESI-MS spectra,
214 UV-vis spectrum, CD spectra, and crystallographic data
215 refinement (PDF)

216 ■ AUTHOR INFORMATION

217 Corresponding Authors

218 *E-mail: antonello.merlino@unina.it.

219 *E-mail: luigi.messori@unifi.it.

220 ORCID

221 Alessandro Pratesi: 0000-0002-9553-9943

222 Damiano Cirri: 0000-0001-9175-9562

223 Dolores Fregona: 0000-0002-8101-1101

224 Antonello Merlino: 0000-0002-1045-7720

225 Luigi Messori: 0000-0002-9490-8014

226 Notes

227 The authors declare no competing financial interest.

228 ■ ACKNOWLEDGMENTS

229 A.M. acknowledges ESRF staff for technical assistance and M.
230 Amendola at the Institute of Biostructures and Bioimages,
231 CNR, Naples, Italy, for preliminary X-ray diffraction data
232 collection experiments. L.M. and A.P. acknowledge Benefi-
233 centia Stiftung, Ente Cassa Rismarmio Firenze, and Associa-
234 zione Italiana per la Ricerca sul Cancro (AIRC) for funding the
235 project “Multi-user Equipment Program 2016” (reference code
236 19650). G.F. thanks AIRC-Fondazione Italiana per la Ricerca
237 sul Cancro (FIRC) for a 3-year fellowship for project code
238 22587. D.C. thanks AIRC and Fondazione CR Firenze for
239 financial support (a 1-year fellowship for Italy; project code
240 22294).

241 ■ REFERENCES

- 242 (1) Larsen, M. T.; Kuhlmann, M.; Hvam, M. L.; Howard, K. A.
243 Albumin-based drug delivery: harnessing nature to cure disease. *Mol.*
244 *Cell Ther.* **2016**, *4*, 3.
245 (2) Fanali, G.; di Masi, A.; Trezza, V.; Marino, M.; Fasano, M.;
246 Ascenzi, P. Human serum albumin: from bench to bedside. *Mol.*
247 *Aspects Med.* **2012**, *33*, 209–290.
248 (3) Gou, Y.; Zhang, Y.; Qi, J.; Chen, S.; Zhou, Z.; Wu, X.; Liang, H.;
249 Yang, F. Developing an anticancer copper(II) pro-drug based on the
250 nature of cancer cell and human serum albumin carrier IIA
251 subdomain: mouse model of breast cancer. *Oncotarget* **2016**, *7*,
252 67004–67019.
253 (4) Ascenzi, P.; di Masi, A.; Fanali, G.; Fasano, M. Heme-based
254 catalytic properties of human serum albumin. *Cell Death Discov* **2015**,
255 *1*, 15025.
256 (5) Ferraro, G.; Massai, L.; Messori, L.; Merlino, A. Cisplatin
257 binding to human serum albumin: a structural study. *Chem. Commun.*
258 **2015**, *51*, 9436–9439.
259 (6) Bijelic, A.; Theiner, S.; Keppler, B. K.; Rompel, A. X-ray
260 Structure Analysis of Indazolium trans-[Tetrachlorobis(1*H*-indazole)-
261 ruthenate(III)] (KP1019) Bound to Human Serum Albumin Reveals
262 Two Ruthenium Binding Sites and Provides Insights into the Drug
263 Binding Mechanism. *J. Med. Chem.* **2016**, *59*, 5894–5903.
264 (7) Aldinucci, D.; Ronconi, L.; Fregona, D. Groundbreaking
265 gold(III) anticancer agents. *Drug Discovery Today* **2009**, *14*, 1075–
266 1076.
267 (8) Nardon, C.; Boscutti, G.; Gabbiani, C.; Massai, L.; Pettenuzzo,
268 N.; Fassina, A.; Messori, L.; Fregona, D. Cell and Cell-Free
269 Mechanistic Studies on Two Gold(III) Complexes with Proven
270 Antitumor Properties. *Eur. J. Inorg. Chem.* **2017**, *12*, 1737–1744.
271 (9) Boscutti, G.; Marchiò, L.; Ronconi, L.; Fregona, D. Insights into
272 the Reactivity of Gold–Dithiocarbamate Anticancer Agents toward

- Model Biomolecules by Using Multinuclear NMR Spectroscopy. *273*
Chem. - Eur. J. **2013**, *19*, 13428–13436. *274*
(10) Merlino, A.; Marzo, T.; Messori, L. Protein Metalation by *275*
Anticancer Metallo-drugs: A Joint ESI MS and XRD Investigative *276*
Strategy. *Chem. - Eur. J.* **2017**, *23*, 6942–6947. *277*
(11) Messori, L.; Merlino, A. Protein metalation by metal-based *278*
drugs: X-ray crystallography and mass spectrometry studies. *Chem.* *279*
Commun. **2017**, *53*, 11622–11633. *280*
(12) Russo Krauss, I.; Sica, F.; Mattia, C. A.; Merlino, A. Increasing *281*
the X-ray Diffraction Power of Protein Crystals by Dehydration: The *282*
Case of Bovine Serum Albumin and a Survey of Literature Data. *Int. J.* *283*
Mol. Sci. **2012**, *13*, 3782–3800. *284*
(13) Majorek, K. A.; Porebski, P. J.; Dayal, A.; Zimmerman, M. D.; *285*
Jablonska, K.; Stewart, A. J.; Chruszcz, M.; Minor, W. Structural and *286*
immunologic characterization of bovine, horse, and rabbit serum *287*
albumins. *Mol. Immunol.* **2012**, *52*, 174–182. *288*
(14) Bujacz, A.; Zielinski, K.; Sekula, B. Structural studies of bovine, *289*
equine, and leporine serum albumin complexes with naproxen. *290*
Proteins: Struct., Funct., Genet. **2014**, *82*, 2199–2208. *291*
(15) Sekula, B.; Zielinski, K.; Bujacz, A. Crystallographic studies of *292*
the complexes of bovine and equine serum albumin with 3,5- *293*
diiodosalicylic acid. *Int. J. Biol. Macromol.* **2013**, *60*, 316–324. *294*
(16) Pratesi, A.; Cirri, D.; Ciofi, L.; Messori, L. Reactions of *295*
Auranofin and Its Pseudohalide Derivatives with Serum Albumin *296*
Investigated through ESI-Q-TOF MS. *Inorg. Chem.* **2018**, *57*, 10507–
10510. *298*
(17) Massai, L.; Pratesi, A.; Bogojeski, J.; Banchini, M.; Pillozzi, S.; *299*
Messori, L.; Bugarčić, Ž. D. Antiproliferative properties and *300*
biomolecular interactions of three Pd(II) and Pt(II) complexes. *J.* *301*
Inorg. Biochem. **2016**, *165*, 1–6. *302*
(18) Michelucci, E.; Pieraccini, G.; Moneti, G.; Gabbiani, C.; Pratesi, *303*
A.; Messori, L. Mass spectrometry and metallomics: A general *304*
protocol to assess stability of metallo-drug-protein adducts in bottom- *305*
up MS experiments. *Talanta* **2017**, *167*, 30. *306*
(19) Biancalana, L.; Pratesi, A.; Chiellini, F.; Zacchini, F.; Funaioli, *307*
T.; Gabbiani, C.; Marchetti, F. Ruthenium arene complexes with *308*
triphenylphosphane ligands: cytotoxicity towards pancreatic cancer *309*
cells, interaction with model proteins, and effect of ethacrynic acid *310*
substitution. *New J. Chem.* **2017**, *41*, 14574–14588. *311*
(20) Talib, J.; Beck, J. L.; Ralph, S. F. A mass spectrometric *312*
investigation of the binding of gold antiarthritic agents and the *313*
metabolite [Au(CN)₂][−] to human serum albumin. *JBIC, J. Biol. Inorg.* *314*
Chem. **2006**, *11*, 559–570. *315*
(21) Messori, L.; Balerna, A.; Ascone, I.; Castellano, C.; Gabbiani, *316*
C.; Casini, A.; Marchioni, C.; Jaouen, G.; Congiu Castellano, A. X-ray *317*
absorption spectroscopy studies of the adducts formed between *318*
cytotoxic gold compounds and two major serum proteins. *JBIC, J.* *319*
Biol. Inorg. Chem. **2011**, *16*, 491–499. *320*
(22) Russo Krauss, I.; Messori, L.; Cinelli, M. A.; Marasco, D.; *321*
Sirignano, R.; Merlino, A. Interactions of gold-based drugs with *322*
proteins: the structure and stability of the adduct formed in the *323*
reaction between lysozyme and the cytotoxic gold(III) compound *324*
Auoxo3. *Dalton Trans* **2014**, *43*, 17483–17488. *325*
(23) Jungwirth, U.; Kowol, C. R.; Keppler, B. K.; Hartinger, C. G.; *326*
Berger, W.; Heffeter, P. Anticancer activity of metal complexes: *327*
involvement of redox processes. *Antioxid. Redox Signaling* **2011**, *15*, *328*
1085–1127. *329*
(24) Witkiewicz, P. L.; Shaw, C. F., III Oxidative cleavage of peptide *330*
and protein disulphide bonds by gold(III): a mechanism for gold *331*
toxicity. *J. Chem. Soc., Chem. Commun.* **1981**, *21*, 1111–1114. *332*
(25) Pacheco, E. A.; Tiekink, E. R. T.; Whitehouse, M. W. In *Gold* *333*
Chemistry; Mohr, F., Ed.; Wiley-VCH: Weinheim, Germany, 2009. *334*
(26) Le Guennec, A.; Tayyari, F.; Edison, A. S. Alternatives to *335*
Nuclear Overhauser Enhancement Spectroscopy Presat and Carr- *336*
Purcell–Meiboom–Gill Presat for NMR-Based Metabolomics. *Anal.* *337*
Chem. **2017**, *89*, 8582. *338*
(27) Nayak, N. C.; Shin, K. Human serum albumin mediated self- *339*
assembly of gold nanoparticles into hollow spheres. *Nanotechnology* *340*
2008, *19*, 265603. *341*